

## Properties of CMR composites<sup>†</sup>

D BAHADUR\* and D DAS

Department of Metallurgical Engineering and Materials Science, Indian  
Institute of Technology, Bombay, Mumbai 400 076, India  
e-mail: dhiren@met.iitb.ac.in

**Abstract.** Colossal magnetoresistance (CMR) composites form an interesting field of study. The intrinsic CMR, governed by the intragrain transport of the conduction electrons through the double exchange, limits its application owing to the high field requirement and generally low transition temperatures. Extrinsic CMR, a function of the intergrain transport between ferromagnetic (FM) particles, plays a crucial role in enhancing low field magnetoresistance (LFMR) or increasing room temperature magnetoresistance. Since extrinsic CMR is a grain boundary controlled phenomena, magnetically dirty grain boundaries in the virgin state of the sample help in achieving a high LFMR or increase the field sensitivity. In this article, we give the properties of different composites of magnetoresistive LCMO or LSMO where the second component is (a) an insulating phase, (b) a conducting phase, (c) a nonmagnetic phase and (d) a magnetic phase. We present here some of our recent work on CMR composites where the CMR phase is chosen as LCMO and SiO<sub>2</sub>, ZnO, ZrO<sub>2</sub> and SiCN have been used as the different second phase of the composites. We summarise some of the salient features of the results.

**Keywords.** Manganites; colossal magnetoresistance; composites.

### 1. Introduction

Perovskite manganites have been the subject of intense research for the last few years because of their inherent potential to exhibit many interesting properties including colossal magnetoresistance (CMR).<sup>1</sup> The work of Jin *et al*<sup>2</sup> triggered many researchers into working in this fascinating field. The intrinsic CMR effect, caused by the 'double exchange' mechanism proposed by Zener<sup>3</sup> in 1951, is useful in explaining mostly intrinsic CMR. Extrinsic CMR is reported to be due to grain boundaries,<sup>4</sup> artificial grain boundaries,<sup>5,6</sup> atomic-size defects in the film-substrate interface<sup>7,8</sup> or nanosized inclusions that appear during the film deposition or postannealing.<sup>9</sup> These are generally ascribed to the spin-polarised intergrain tunnelling of conduction electrons as proposed by Hwang *et al*<sup>10</sup>. The tunnelling process takes place across the interfaces or grains separated by an energy barrier related to the magnetic disorder. Hence dilution with an insulating material in the manganites adjusts the barrier layer and thus influences the tunnelling process. Since these extraneous effects act as pinning centres in remagnetisation by domain wall displacement, a small field will aligns the neighbouring FM grains and hence an enhanced MR response is achieved at low fields and low temperatures. Therefore, a spin misorientation at the magnetically virgin state of the system is crucial to obtain an

<sup>†</sup>Dedicated to Professor C N R Rao on his 70th birthday

\*For correspondence

enhanced MR. This extrinsic effect is observed in a wide temperature range, at low field  $B \leq 1$  kOe and makes it more useful from the application point of view.

Although spin-polarised tunnelling through the grain boundary leads to high MR at low fields corresponding to a composition called the percolation threshold for the composite system, its magnitude falls rapidly with temperature. Several workers have attempted to enhance the low temperature low-field MR (LFMR) or the room-temperature MR by making a composite of these CMR oxides like  $\text{La}_{0.67}\text{Ca}_{0.33}\text{MnO}_3$  (LCMO) or  $\text{La}_{0.67}\text{Sr}_{0.33}\text{MnO}_3$  (LSMO) with a secondary phase like an insulating oxide, a hard ferromagnetic material or a polymer material etc. But in each case, the basic objective is to increase the height of the tunnel barrier between the neighbouring FM grains. The area of composite of CMR materials is still very young and hence it is important that before we discuss some of our own work, we give a summary of what has been done in this field in last 3–4 years.

## 2. General behaviour of CMR composites

The earliest work reported in the area of CMR composites was by Li Balcells *et al*<sup>11</sup> and Petrov *et al*<sup>12</sup> in 1999. Li Balcells *et al*<sup>11</sup> have studied the magnetoresistance of  $x\text{LSMO}/(1-x)\text{CeO}_2$  composite ( $x = 100, 80, 60, 40, 30, 25, 20$  vol.%) as a function of metal/insulator composition, temperature and magnetic field and have found a dramatic enhancement of LFMR for samples close to the metallic percolation threshold. The improved field sensitivity is fairly large even at room temperature. They observed two peaks in the resistivity curve and a resistivity rise by 6–7 orders of magnitude at the percolation threshold,  $x_p = 20\%$  and a LFMR of about 1.5% at  $H = 100$  Oe at 300 K. A broad peak in the resistivity curve at around 250 K has been attributed to the bad interparticle contacts. But the LFMR response, due to intergrain coupling, at  $x = x_p$  is very poor. The high field response has been attributed mainly to the magnetic and electrical characteristics of the grains themselves. Petrov *et al*<sup>12</sup> have studied the electrical and magnetic transport properties of  $x\text{LCMO}/(1-x)\text{SrTiO}_3$  ( $x = 10\text{--}100$  vol.%) composites. A high field MR as well as LFMR close to percolation threshold,  $x_c = 60\%$  is attributed due to increased disorder in the grain boundary and is almost over an order of magnitude higher than the corresponding pure LCMO value. The resistivity goes up by 6 orders of magnitude above  $x_c$ . MR also increases with  $x$  and becomes maximum at  $x = x_c$  and then goes down. Magnetisation curve with temperature shows an upturn below 50 K and does not saturate up to 50 kOe, which has been ascribed to the highly disordered nonmagnetic interfacial region. Composites with other insulating materials like yttria-stabilised zirconia (YSZ),<sup>13</sup> silica ( $\text{SiO}_2$ ),<sup>14</sup> alumina ( $\text{Al}_2\text{O}_3$ )<sup>15,16</sup> are also reported.  $(\text{LSMO})_{1-x}/(\text{YSZ})_x$  composites with varying  $x$  (0.0 to 5%) have been investigated by Xia and his co-workers.<sup>13</sup> Broadening of  $T_C$  and shifting of  $T_{\text{MI}}$  to lower temperatures are observed. But  $T_{\text{MI}}$ , interestingly decreases up to  $x \leq 2\%$  and then it increases. Room temperature MR of the composites is higher compared to pure LSMO at 3T field. They did not find any percolation threshold in the system. The transport and magnetic properties have been explained on the basis of the reaction products between LSMO and YSZ. They have proposed a two-channel conduction model for the composites. Low temperature MR rise is due to spin-polarised tunnelling through the LSMO grains but  $\text{La}_2\text{Zr}_2\text{O}_7$ ,  $\text{SrZrO}_3$  along with YSZ (reaction products between the components) impairs the transport properties for low  $x$  by segregating as thin channel of insulating layer in the grain boundaries of the LSMO phase.  $(\text{LSMO})_{1-x}/(\text{SiO}_2)_x$  for  $x = 0.0\text{--}1.0$  mol.% com-

posites show resistivity rise with increasing  $x$  and shifting of  $T_{MI}$  towards lower temperatures as observed by Huang *et al.*<sup>14</sup> In this case the MR behaviour of the composite is superior at  $T > 150$  K but inferior for  $T < 150$  K. MR at 300 K is 21.4% for  $x = 0.20$  but 17.7% for  $x = 0.0$  at 50 kOe field. Spin-polarised tunnelling through the LSMO grains in the presence of the insulating  $\text{SiO}_2$  in the grain boundary is ascribed for the observed effect. Another insulating inert material  $\text{Al}_2\text{O}_3$ , used for the junction MR devices, has been used by Hueso *et al.*<sup>15</sup> to form the composite  $(\text{LCMO})_{1-x}(\text{Al}_2\text{O}_3)_x$  ( $x = 0.0\text{--}25$  vol.%). They have seen a threshold percolation at  $x = 10$  vol.%. Resistivity rises by 3 orders of magnitude with increasing  $x$  at 100 K and shift of the transition temperature towards lower temperature is seen as usual like other CMR composites. But no metal–insulator transition is observed for  $x \geq 8\%$ . The resistivity behaviour throughout the whole temperature range is fitted based on a two-channel conduction model. They have observed the MR maximum at the conduction threshold ( $x = 10\%$ ) at 77 K and at 7.5 kOe.  $(\text{LSMO})_{1-x}/(\text{MgO})_x$  ( $x = 0.0\text{--}0.5$ ) composites exhibit a pronounced LFMR compared to pure LSMO which is  $< 1\%$  at  $B \leq 1$  kOe at low temperatures. For  $x = 0.05$ , MR is 25% at  $T = 4.2$  K and at 50 kOe field. Even a small amount of MgO ( $x \leq 0.05$ ) changes the intrinsic metallic bulk electron transport into a grain boundary controlled extrinsic behaviour.<sup>17</sup> HFMR is also increased up to 50–60% in the range 4.2–200 K at 50 kOe. In case of  $(\text{LSMO})_x/(\text{SrMeO}_3)_{1-x}$  composite<sup>18,19</sup> (Me = Ti, Zr,  $x = 20\text{--}70$  mol.%) the MR enhancement point ( $x = \text{mol.}\%$  LSMO) is dependent on the annealing temperature. For LSMO/SrTiO<sub>3</sub> it is 1.5% at  $H = 100$  Oe and at  $T = 298$  K and that for LSMO/SrZrO<sub>3</sub> it is 2.5% at the same field and temperature. Also the variation of MR with  $x$  shows the same trend as that of coercive field with  $x$ . Yan *et al.*<sup>20</sup> have investigated the LFMR of the LSMO/CoFe<sub>2</sub>O<sub>4</sub> composite for a single composition of 20 wt% CoFe<sub>2</sub>O<sub>4</sub>. The resistivity of the composite is about an order of magnitude larger than that of the same grain-sized pure LSMO. A large LFMR has been obtained in this composite compared to pure LSMO. At 5 kOe, the MR of 20 wt% composite is 10% at 280 K and 5% at 290 K whereas these values for pure LSMO are 2 and 1% respectively. The high resistivity of the composite is attributed to the random scattering of the spin electrons at the surfaces of the magnetic CoFe<sub>2</sub>O<sub>4</sub> grains. Since the spin-dependent scattering of the conduction electrons at the grain boundaries is highly field sensitive, the magnetic scattering of the polarised charge carriers may be responsible for the LFMR. Another interesting system with a hard ferromagnetic insulator (HFMI) as the second phase of the composite is reported by Huang *et al.*<sup>21</sup> They have studied  $(\text{L}_{0.67}\text{Sr}_{0.33}\text{MnO}_3)_{1-x}/(\text{BaFe}_{11.3}(\text{ZnSn})_{0.7}\text{O}_{19})_x$  (BAM) composites as a function of vol.% (0.0–1.0) of the insulating phase. A resistivity rise with increasing  $x$ , indicates a percolative system. But in contrast to the other FMM/HFMI composite discussed earlier they have reduced LFMR whereas HFMR slopes in the  $r$  vs  $H$  curve are greater. Based on this observation, they suggest that magnetic coupling is not solely responsible for increase in MR at low field, but microstructure also plays an important role to have the desired effect. Gupta *et al.*<sup>22</sup> have reported the magnetotransport studies of LSMO–borosilicate glass composites. They have reported an enhanced LFMR of about 1.8% at 200 Oe at room temperature for 25 wt% of glass, the percolation threshold composition for the system. They have further argued that the glass layer, as an amorphous insulator, seats within the grain boundaries of the LSMO and acts as a barrier for spin-polarised tunnelling thereby enhancing the LFMR. They have also found the sudden resistivity jumps around the percolation threshold. The broad peak in the resistivity curve is understood on the basis of a parallel resistor model where the sample is considered to be made of a parallel network of

conducting and insulating paths. The sharp drop of resistivity in MR vs  $H$  curve is attributed to the much-discussed spin-polarised tunnelling through the FM grain boundaries whereas the gradual drop thereafter is assigned to the magnetically hard region at the disordered interface.

(LCMO)<sub>1-x</sub>(polyparaphenylene, PPP)<sub>x</sub> ( $x$  = wt. fraction, 0.0–0.6) composites<sup>23</sup> have been studied by Huang and his group. MR enhances significantly at lower temperatures for the composite, which is 3 times larger than pure LCMO. But this MR enhancement point ( $x$ ) is not the same as that of the percolation threshold derived from  $\rho$  vs  $x$  curve.  $T_{MI}$  for the composites shifts to the lower temperature by 56 K for  $x = 0.1$  from 172 K for pure LCMO which is much less than the corresponding magnetic transition temperature,  $T_C$  and has been attributed to the grain boundary dominated transport. Resistivity increases almost by 5 orders of magnitude at the percolation threshold composition. PPP being not able to form a thin enough layer between the LCMO grains (seen from the micrograph) could not act as a tunnelling barrier and hence could not change the tunnelling conduction through them. But it possibly induces a spin disorder at the LCMO surface and certainly changes the magnetic ordering at the grain boundary. Similar studies have been carried out by Yan *et al.*<sup>24</sup> for the (LSMO)<sub>1-x</sub>(PPP)<sub>x</sub> composites (wt. fraction of PPP,  $x = 0.0, 0.2, 0.6, 1.0$ ). They have found a remarkable LFMR especially at low temperature and at  $H < 5$  kOe.

The magnetoresistance of (La<sub>0.7</sub>Ca<sub>0.3</sub>MnO<sub>3</sub>)<sub>0.5</sub>/(La<sub>0.7</sub>Sr<sub>0.3</sub>MnO<sub>3</sub>)<sub>0.5</sub> composite<sup>25</sup> has been investigated as a function of sintering temperature. Raising the sintering temperature triggers the interfacial reaction between LCMO and LSMO which dictates the MR property over a wide temperature range across the room temperature. The resistivity of the composite goes on decreasing with sintering temperature. This has been attributed to the presence of the new reaction product, La<sub>0.7</sub>Ca<sub>0.15</sub>Sr<sub>0.15</sub>MnO<sub>3</sub>, which is a low resistivity component compared to pure LCMO, keeping in mind the parallel circuit model for the composites. MR width of about 60 K around  $T_{MI}$  rises to about 120 K for the sample sintered at 1300°C. The coexistence of multiphase in the interface associated with the chemical and magnetic inhomogeneity is the probable cause of the broad MR response across the room temperature as suggested by the authors. Another such composite studied is (LSMO)<sub>1-x</sub>/(Sm<sub>0.7</sub>Sr<sub>0.3</sub>MnO<sub>3</sub>)<sub>x</sub> (SSMO)<sup>26</sup> with  $x = 0.0$ – $1.0$ . Since the transition temperature for SSMO is 63 K, it behaves as a paramagnetic insulator at high temperature and the combination effectively acts as a FM-insulator composite. The resistivity increases by two orders of magnitude with increasing SSMO content, shifting  $T_{MI}$  towards lower temperatures for the composites. Maximum MR of 28.3% is obtained at 293 K for  $x = 0.6$  (percolation Threshold) which rises to 46.4% at 200 K for  $x = 0.7$  and at 50 kOe. Observed LFMR is attributed due to spin-polarised tunnelling through the LSMO grains but the HTMR enhancement is because of enhanced magnetic disorder due to the presence of PM SSMO in LSMO grain boundaries which leads to the blocking of spin-coupling between the neighbouring LSMO grains and hence improved HTMR. Composites such as (LSMO)<sub>1-x</sub>/(Pr<sub>0.5</sub>Sr<sub>0.5</sub>MnO<sub>3</sub>)<sub>x</sub> (PSMO) with  $x = 0.0$ – $1.0$  have been studied by Liu *et al.*<sup>27</sup> and Yuan *et al.*<sup>28</sup> Resistivity increases and  $T_{MI}$  shifts to lower temperatures with increasing  $x$  and has been explained in terms of spin-coupling layer inside LSMO grains.

A ferromagnetic/metal type composite (LCMO/Ag) has been investigated by Huang *et al.*<sup>29</sup> and a large enhancement in MR near room temperature and a dramatic decrease in resistivity for the composite has been reported. They have observed a shifting of  $T_{MI}$  towards  $T_C$  in Ag-melted LCMO and suggested magnetic inhomogeneity near the LCMO

grain boundaries which are responsible for enhanced MR near room temperature.  $(\text{LCMO})_{1-x}\text{Ag}_x$  ( $x=0.10$ ) composite, where  $x$  is the nominal wt. fraction, shows two unreacted phases.  $M$  vs  $T$  shows no change in  $T_C$  which rules out the possibility of any Ag incorporation into the LCMO lattice.  $T_{MI}$  shifts to higher temperatures and resistivity of the system falls with calcination temperature. A second broad peak at around 140 K for the sample calcined at 600°C in  $\rho$  vs  $T$  curve is ascribed to the extrinsic behaviour of the system which might be related to the insufficient crystallisation of the Ag in the system as suggested by the authors. Although the low temperature MR of the composites is lower than that of pure LCMO, HTMR are significantly higher around the room temperature. MR ratio at 300 K is 15% for pure LCMO ( $x=0.0$ ), 18 and 23% for the samples with  $x=0.10$  calcined at 700 and 1000°C respectively. The authors argue that Ag imparts the magnetic inhomogeneity in LCMO grain boundaries and in melted condition (at  $T_{Ag}=1000^\circ\text{C}$ ) it provides a conduction channel, improving the grain connectivity and hence influence the transport property. Therefore a cooperative effect of magnetic inhomogeneity and transport connectivity at the LCMO grain boundaries improve the room temperature MR of the composites. The magnetic, transport and structural properties of another FM-metallic bulk polycrystalline composites of  $\text{La}_{0.833}\text{Na}_{0.167}\text{MnO}_3$  and  $\text{Ag}_2\text{O}$  with molar proportion 1 :  $x(0.0-0.5)$  has been investigated by Tang *et al.*<sup>30</sup> Observations are much more like that of LCMO/Ag composites. This is because of high temperature sintering of the composites.  $\text{Ag}_2\text{O}$  gets reduced to metallic Ag and gets populated at the grain boundaries of the perovskite manganites. Room temperature MR of the composites improves. It is 27% at 11.5 kOe for  $x=0.25$ . Although there is no signature of percolation threshold composition of the composite in  $\rho$  vs  $T$  curve, MR shows a maxima at  $x=0.25$ . Instead of rise in resistivity with addition of a second phase in the composites,  $\text{Ag}_2\text{O}$  decreases the resistivity of the system by improving the connectivity between the FM grains. MR vs  $H$  behaviour shows linear increment of MR with  $H$  without saturation even up to 11.5 kOe. Spin-dependent scattering at the grain boundaries of the FM component is basically responsible for the observed effect.

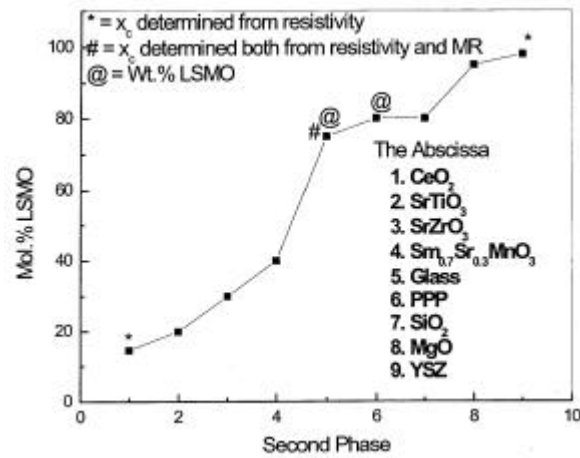
A tuning between positive and negative MR is observed in  $(\text{LSMO})_{1-x}(\text{La}_{1.85}\text{Sr}_{0.15}\text{CuO}_4)_x$  (LSCO) ( $x = \text{wt. fraction, } 0.0-0.9$ ) composites,<sup>31</sup> a composite between a CMR and a superconducting component. Above the superconducting transition of LSCO all samples show negative MR up to room temperature for  $x < 0.5$ . But as the applied field increases a positive MR comes into picture for samples with  $x > 0.5$  because of the magnetic breakdown of the superconducting coupling within LSCO grains. This magnetic field and composition sensitive competition between the positive and negative MR reveals the coexistence of a ferromagnetic and superconductive ordering in the system that favours the materials to be used as a magnetic field sensitive device like vortex detector. But it limits its applicability only in the low temperature because for the superconductive ordering the material must have to be subjected below the superconducting transition temperature ( $T_{SC}$ ) of LSCO. The summary of the magnetic and electrical transport properties of the reported CMR composites near their threshold compositions and which are discussed above is given in table 1. The variation of the percolation threshold composition,  $x_C$  in terms of mol.% of LSMO and LCMO with different second phases has been shown in figures 1 and 2 respectively. Though it is difficult to derive any clear inferences from this table and the two figures, but it may serve as a good guide for the researchers in this area.

**Table 1.** The magnetic and electrical transport parameters of the reported CMR composites near the threshold compositions.

LS =  $\text{La}_{0.7}\text{Sr}_{0.3}\text{MnO}_3$ ; LC =  $\text{La}_{0.7}\text{Ca}_{0.3}\text{MnO}_3$ ; LN =  $\text{La}_{0.833}\text{Na}_{0.167}\text{MnO}_3$ ; SS =  $\text{Sm}_{0.7}\text{Sr}_{0.3}\text{MnO}_3$ ; IN = insulating; NM = non-magnetic; CN = conducting; MG = magnetic

Composite system	Nature of 2nd phase	$x_c$ (mol.%)		$T_C$ (K)	$T_{MI}$ (K)	$r_{MI}$ ( $\Omega$ cm)/ $R$ ( $\Omega$ )		MR (%) at $x_c$ (kOe, K)	Ref.
		LS/LC							
LS/SrTiO <sub>3</sub>	IN, NM	20 (1)		–	–	–	–	1.5 (0.1, 298)	17
LS/SrZrO <sub>3</sub>	IN, NM	30 (1)		–	–	–	–	2.5 (0.1, 298)	17
LC/SrTiO <sub>3</sub>	IN, NM	60.9 (2)		310	100	$165 \cdot 10^2$		$6^\#$ (0.5, 75)	15
LS/MgO	IN, NM	95 (1)		310	175 (broad)	10,000 $\Omega$		25 (50, 4.2)	16
LS/CeO <sub>2</sub>	IN, NM	14.63 (2)		–	–	–	–	1.5 (0.1, 300)	10
LS/SiO <sub>2</sub>	IN, NM	80 (1)		–	225	6.5 $\Omega$		21.4 (50, 300)	12
LS/YSZ	IN, NM	98 (2)		–	338	–	–	20 (30, 300)	11
LC/Al <sub>2</sub> O <sub>3</sub>	IN, NM	86.6 (1,2)		265	Not found	$> 100^\circ$		43 (7.5, 77)	13, 14
LS/SS	CN, MG	40 (1)		–	$\sim 125$	$< 100^\circ$		$28.3^\#$ (50, 293)	25
LN/Ag <sub>2</sub> O	CN, NM	80 (1)		–	–	–	–	27 (11.5, 300)	29
LS/PPP	IN, NM	80* (1)		–	Not found	$\sim 10^{1.5^\circ}$		14 (50, 300)	23
LC/PPP	IN, NM	60* (2)		272	Not found	$\sim 10^{3.5^\circ}$		$10^\#$ (50, 260)	22
LS/Glass	IN, NM	75* (1,2)		–	–	–	–	1.8 (0.2, 298)	21

(1)  $x_c$  determined from MR measurement; (2)  $x_c$  determined from resistivity measurement; (1, 2)  $x_c$  determined from both resistivity and MR measurement; \*Wt.% LS/LC;  $^\#$ MR is taken as  $(r_0 - r_H)/r_H$ ;  $^\circ$  estimated from the figures in the respective references

**Figure 1.** Variation of percolation threshold composition in terms of LSMO mol.% (y axis) with different second phases (x axis) for the LSMO composites.

### 3. Present investigations

We have investigated some CMR composite systems involving  $\text{La}_{0.67}\text{Ca}_{0.33}\text{MnO}_3$  as the ferromagnetic phase and  $\text{SiO}_2$  (insulating refractory oxide), ZnO (a well-known semi-conducting material), SiCN (a conducting polymer-derived ceramic, PDC) and  $\text{ZrO}_2$  (an ionic conductor) as the second phase of the composites. Si being strongly preferred for

tetrahedral coordination cannot enter the perovskite lattice. So at best what it can do is either react with LCMO to form another phase or precipitate as  $\text{SiO}_2$  or some derivative of this in the grain boundary region. SiCN is conducting, so differs in transport properties from  $\text{SiO}_2$ . ZnO itself being a semiconducting material should influence the transport properties of conducting LCMO in a different way than the insulating materials like  $\text{SiO}_2$  or  $\text{ZrO}_2$ . Zn also prefers tetrahedral coordination although octahedral coordinated Zn is also reported in the CMR literature where it substitutes Mn in the LCMO/LSMO lattice.  $\text{ZrO}_2$  is a well-known ionic conductor. In the polycrystalline bulk synthetic route it is difficult for  $\text{Zr}^{+4}$  to go into the manganite perovskite lattice (B sites) because of large size mismatch.<sup>32</sup> Moreover  $\text{Zr}^{+4}$  does not prefer octahedral coordination.

Most composite samples, except with SiCN, are prepared by a citrate gel route.<sup>33</sup> For LCMO:  $x\text{SiO}_2$  ( $x = 0.0\text{--}0.30$  mol.%) composites tetraethoxyorthosilicate (TEOS) has been used as the source of  $\text{SiO}_2$ , which is also a good gelating agent. For LCMO:  $x\text{ZnO}$  composites ( $x = 0.0\text{--}0.30$  mol.%), commercially available ZnO powders have been used as the second phase of the composites. For LCMO:  $x\text{ZrO}_2$  composites<sup>34</sup> ( $x = 0.0\text{--}0.80$  mol.%) zirconium oxychloride,  $\text{ZrOCl}_2 \cdot 8\text{H}_2\text{O}$  has been chosen as the starting material for  $\text{ZrO}_2$  in the composites. But in case of LCMO:  $x\text{SiCN}$  composites ( $x = 0.0\text{--}0.40$  vol.%), SiCN, a polymer-derived ceramics (PDC) has been derived from its commercially available liquid polymer precursor ceraset. Heat treatment of ceraset at  $400^\circ\text{C}$  for 5 h in flowing- $\text{N}_2$  gas atmosphere leads to the cross linking of the polymer. The subsequent pyrolysis of cross-linked polymer, after ball milling in an attrition mill, at  $1500^\circ\text{C}$  for 10 h. in flowing- $\text{N}_2$  gas atmosphere results in the pyrolysed powder of SiCN which is basically a mixture of  $a\text{Si}_3\text{N}_4$ ,  $a\text{SiC}$  and  $b\text{SiC}$ . Mechanical mixture of pyrolysed SiCN and citrate gel derived LCMO, followed by subsequent pelletization in a uniaxial hydraulic press and sintering at  $1100^\circ\text{C}$  for 2 h in a muffle furnace in static air leads to sintered pellets ready for characterisation. Except for the LCMO: SiCN composites, all the composites are synthesised in such a way that the second phase (TEOS, ZnO or  $\text{ZrOCl}_2 \cdot 8\text{H}_2\text{O}$ ) is directly dissolved in the aqueous solution to form the

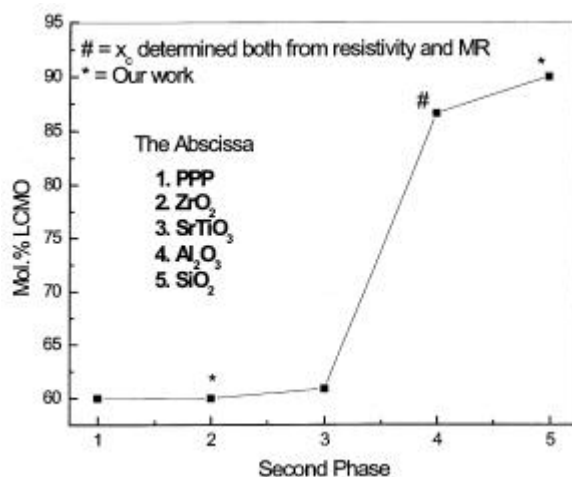


**Figure 2.** Variation of percolation threshold composition in terms of LCMO mol.% (y axis) with different second phases (x axis) for the LCMO composites.

gel to ensure a homogeneous distribution of the second phase in the matrix. On subsequent drying of the gel at 200°C for 24 h leads to precursor powders for the composites. Precursor powders on calcinations at 800°C for 2 h in static air, followed by pelletization and heat treatment at different temperatures in static air gives the final sintered pellets for characterisation.

### 3.1 Properties of LCMO: $x\text{SiO}_2$ composites

LCMO:  $x\text{SiO}_2$  composites show  $\text{Ca}_2\text{La}_8(\text{SiO}_4)_6\text{O}_2$ , an insulating silicate phase along with LCMO phase in the composites and whose amount increases with increasing  $x$ . For  $x = 0.30$ , some  $\text{g-Mn}_2\text{O}_3$  reflections are also seen, along with the other two phases mentioned above. Magnetisation versus temperature measurements at 5 kOe from 5–300 K reveals no shift in  $T_C$  indicating that  $\text{Si}^{+4}$  does not enter the perovskite lattice, as shown in figure 3. The saturation magnetisation at 5 K gradually decreases with  $x$  (seen in figure 3b) as expected because of the magnetic dilution of the system in presence of nonmagnetic silicate phase mentioned earlier. A small hump appears just below 50 K in the  $M$  vs  $T$  curve and which gets prominent as  $x$  increases from 0.05 to 0.30. Such behaviour is also seen earlier with other systems.<sup>16,35–37</sup> Ju and Sohn<sup>38</sup> have explained it on the basis of local microscopic magnetic inhomogeneities arising from the variation in the Mn oxidation state. Gebhardt *et al*<sup>35</sup> in their work on Ce-doped LSMO systems, explained this kink on the basis of the presence of paramagnetic  $\text{MnO}_2$  phase in the compound. In our samples although we did not find any  $\text{MnO}_2$  some  $\text{g-Mn}_2\text{O}_3$  is seen for higher values of  $x$  whose paramagnetic to spin glass transition at around 50 K could be responsible for the observed effect.<sup>39</sup> Resistivity behaviour of the composites with temperature is shown in figure 4a, while figure 4b shows the variation of room temperature resistivity with compositions. All the curves show two peaks. One sharp peak close to their ferromagnetic transition temperature,  $T_C$ , corresponds to their respective metal insulator transition ( $T_{\text{MI}}$ ) (indicated by an arrow), which does not change with composition,  $x$ . But the broad peak appears below the metal–insulator transition and gets prominent as  $x$  increases. This kind of behaviour can be explained based on the scattering mechanism at different temperature region which has been discussed in detail

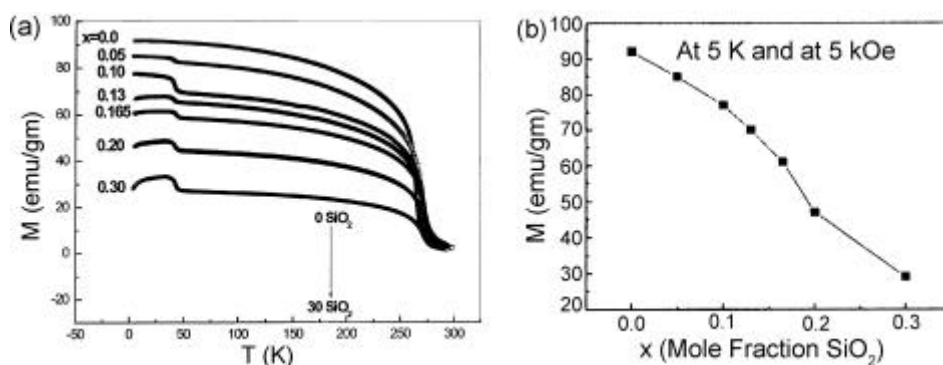


**Figure 3.** (a) Magnetisation behaviour of the  $\text{SiO}_2$  composites with temperature. (b) Shows the saturation magnetisation variation with compositions at 5 K and at 5 kOe field.

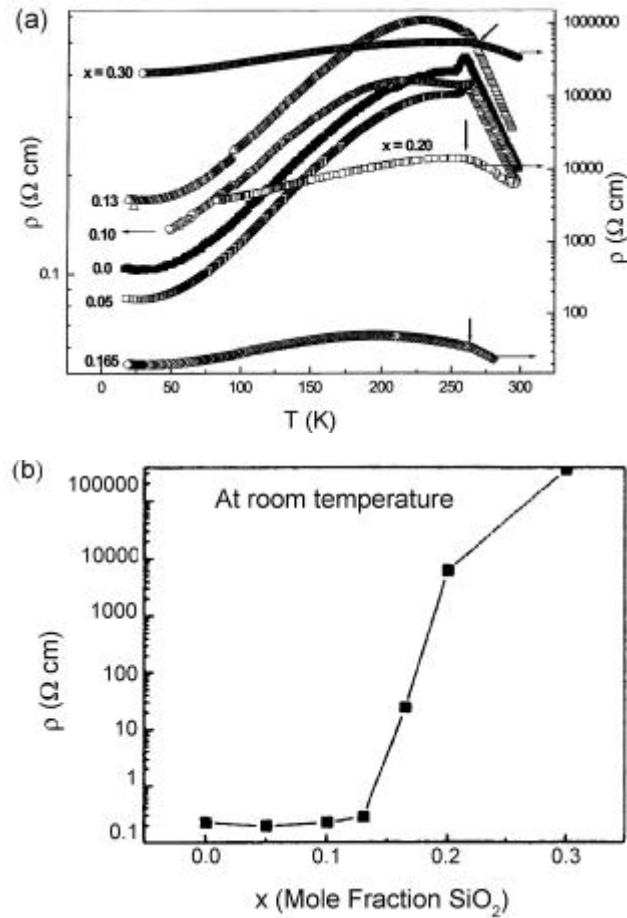


**Figure 4.** (a) Variation of zero field resistivity with temperature for  $\text{SiO}_2$  composites. The plot is in log scale. Right Y axis is for  $x = 0.20, 0.25$  and  $0.40$ . (b) Room temperature resistivity behaviour with composition.

in our earlier work.<sup>39</sup> The sharp transition which is composition ( $x$ ) independent is the result of spin-spin scattering. Since the spins of the magnetic ions ( $\text{Mn}^{+3}$  and  $\text{Mn}^{+4}$ ) get properly aligned at the transition temperature, the resistivity sharply drops leaving behind the signature of the sharp peak. Beyond the transition, the resistivity is primarily governed by the phonon scattering and the temperature independent part in the lower temperature region is the result of impurity scattering. As  $x$  increases, the impurity phases (silicate and  $\text{Mn}_2\text{O}_3$ ) increase in volume as has been shown in figures 5 and 6 and control the overall transport properties of the system. This is the reason why the sharp peak in the resistivity curve disappears slowly and the temperature independent broad peak becomes prominent as  $x$  increases. Room-temperature resistivity increases slowly with composition for lower  $x$  ( $x \leq 0.10$ ) but for  $x \geq 0.13$  it suddenly shoots up and reaches almost six orders of magnitude higher for  $x = 0.30$ , compared to  $x = 0.0$  signalling a percolation threshold composition at  $x = 0.10$  for the composite system. Since the overall resistivity

of this kind of system is considered to be a parallel combination of low resistivity metallic (FM LCMO grains) and a high resistivity insulating silicate phase, we ascribe the broad peak to the intergrain transport between the LCMO grains. With application of the magnetic field (8 kOe) the sharp peak disappears but the broad peak still remains. The plot of MR vs  $T$  (not shown here) has two components, a maxima near  $T_C$  and a low temperature rise irrespective of the compositions,  $x$ . The maxima near  $T_C$  is certainly due to the intrinsic MR inside the LCMO grains and the low temperature rise is because of the magnetic field-induced suppression of the spin-dependent scattering of the conduction electrons. This is similar to the spin-polarised tunnelling of the conduction electrons across the LCMO grain boundaries as proposed by Hwang *et al.*<sup>10</sup>

### 3.2 Properties of LCMO: $x\text{ZnO}$ composites

XRD patterns of the composites show no lines of ZnO even up to  $x = 0.10$  but beyond that ZnO reflections are also seen along with the LCMO lines suggesting that as  $x$  increases from  $x \geq 0.10$ , ZnO separates out from the system and segregates as a separate phase in the system. Magnetisation data support the X-ray observations. Magnetisation behaviour (at 5 kOe) of the samples with temperatures shows a shift of  $T_C$  from 264 K (for  $x = 0.0$ ) to 240 K (for  $x = 0.05$ ) and then to 227 K (for  $x = 0.10$ ). This indicates the incorporation of Zn into the perovskite lattice.<sup>40</sup> Considering the size factor,  $\text{Zn}^{+2}$  substitutes  $\text{Mn}^{+4}$  in the LCMO lattice and hence shifts the transition temperatures. But for

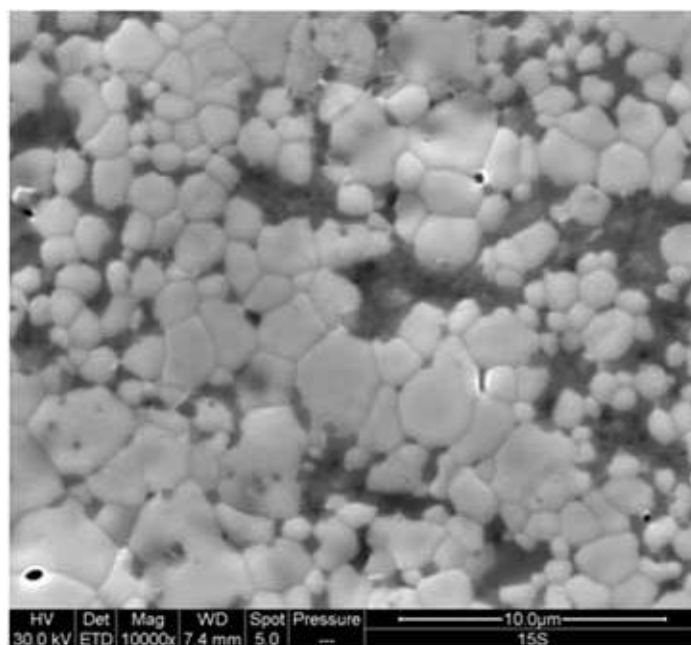


**Figure 5.** Scanning electron micrograph of LCMO:  $x\text{SiO}_2$  ( $x = 0.13$ ) composite sintered at  $1200^\circ\text{C}$  for 2 h. The bright particles are of LCMO and the dark region is the insulating phase.

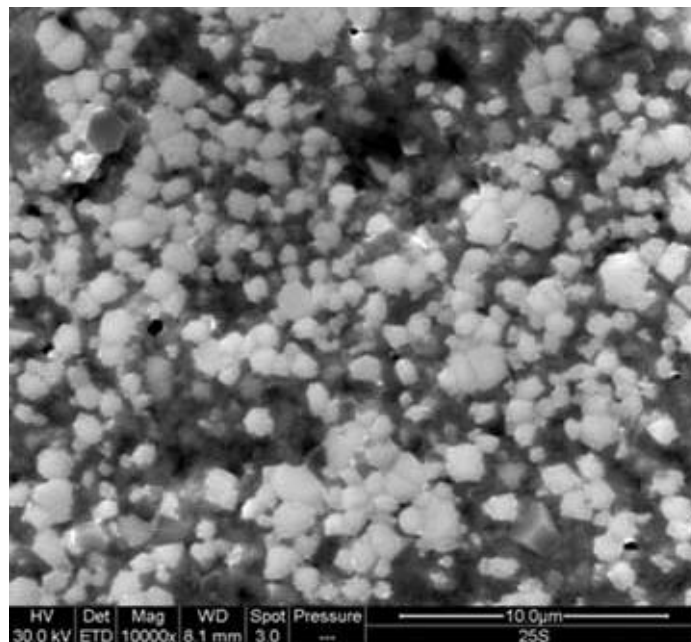


**Figure 6.** Scanning electron micrograph of LCMO:  $x\text{SiO}_2$  ( $x = 0.20$ ) composite sintered at  $1200^\circ\text{C}$  for 2 h. The increase in the amount of insulating phase and the poor interparticle contact with increasing  $x$  is clearly evident from the microstructure.

$x \geq 0.13$ ,  $T_C$  does not change and remains around 225 K indicating that it segregates as a separate phase in the system. Saturation magnetisation at 5 K gradually falls with  $x$  and almost equals to the corresponding fraction of magnetic LCMO in the composite indicating no extra magnetic interaction between the LCMO and the nonmagnetic ZnO present in the system as the second phase of the composites. The zero-field resistivity of the samples increases with  $x$  up to  $x = 0.13$  and thereafter it decreases as  $x$  increases further. All the composites show metal–insulator transition close to their ferromagnetic transition temperature and it shifts from 262 K for  $x = 0.0$  to 216 K for  $x = 0.10$  and then it remains constant at around 217 K for the other composites supporting the X-ray and VSM data. Room temperature or the peak resistivity at  $T_{MI}$  does not increase that much as is observed in case of  $\text{SiO}_2$  composites. Although two orders of magnitude increase in resistivity for  $x = 0.13$  is noticed compared to pure LCMO, no percolation is observed in this case. If Zn substitutes Mn in the perovskite lattice, being a bivalent ion it cannot participate in the double exchange (DE) mechanism involving  $\text{Mn}^{+3}$  and  $\text{Mn}^{+4}$  ions through  $\text{Mn}^{+3}\text{--O--Mn}^{+4}$  network, so in effect it dilutes the DE process and hence the resistivity increases initially up to  $x = 0.15$ . Also  $\text{Zn}^{+2}$  at Mn site, being a bigger ion, should compress some  $\text{Mn}^{+3}\text{--O--Mn}^{+4}$  bonds which in turn would lead to bond angle distortion ( $< 180^\circ$ ) and deteriorate the transport properties as suggested by Ghosh *et al.*<sup>41</sup> But since  $\text{Zn}^{+2}$  can not acquire a higher valent state it induces a higher residence time of the higher valent Mn ion viz  $\text{Mn}^{+4}$  in its close vicinity thereby causing a local charge ordering. The local charge ordering in turn would straighten out some  $\text{Mn}^{+3}\text{--O--Mn}^{+4}$

bonds in its immediate neighbourhood and make the  $\text{Mn}^{+3}\text{-O-Mn}^{+4}$  angle close to  $180^\circ$ , releasing strain in the system which would lead to improved conductivity of the system. This effect becomes prominent for  $x \geq 0.30$  and the same effect is reflected in the MR data also. The MR with temperature shows a peak near their magnetic transition temperature caused by the intrinsic CMR effect. The low temperature rising part is due to spin-dependent scattering at the grain boundaries of the LCMO phase and is the manifestation of the extrinsic CMR effect in the system.

### 3.3 Properties of LCMO: $x\text{ZrO}_2$ composites

The room-temperature X-ray diffraction patterns of LCMO:  $x\text{ZrO}_2$  ( $x = 0.0\text{--}0.80$ ) composites show the presence of  $\text{CaZrO}_3$  and  $m\text{-ZrO}_2$  along with LCMO lines for  $x \leq 0.10$  and for  $x \geq 0.20$ , the composite shows the presence of  $\text{La}_2\text{Zr}_2\text{O}_7$  and  $t\text{-ZrO}_2$  along with LCMO. But the cubic symmetry of LCMO is preserved in all the samples. Low field  $dc$  susceptibility measurement (done by a Quantum Design MPMS 7 SQUID magnetometer) shows (figure not shown) the shifting of the ferromagnetic transition temperature towards the lower temperature for  $x = 0.05$  and then it gradually increases as  $x$  increases further for  $x \geq 0.10$ . The deviations from nominal cation stoichiometry in LCMO, due to the reaction between LCMO and  $\text{ZrO}_2$ , could be the probable reason for the observed effect. The same effect is reflected in their transport properties also. The zero field resistivity behaviour from 4–375 K for the composites is shown in figure 7a and the same for the pure compound is in figure 7b. The peak resistivity (at  $T_{\text{MI}}$ ) initially increases for  $x = 0.05$  compared to pure LCMO ( $x = 0.0$ ) and then it reduces gradually up to  $x = 0.40$ . Again it starts rising for  $x \geq 0.40$  and shows a sudden jump by six orders of magnitude compared to pure LCMO at  $x = 0.80$ . The variation of room temperature resistivity ( $\rho_{\text{RT}}$ ) with the composition ( $x$ ) is shown in figure 7c, indicating a percolation threshold at around  $x = 0.40$ . Although the reaction products between LCMO and  $\text{ZrO}_2$  are insulating in nature, they impart a low resistance to the system which is very surprising. This kind of behaviour is seen earlier<sup>12,42</sup> by many authors and has been explained on the basis of the distribution of the second phases in the LCMO matrix.  $\text{ZrO}_2$  in the lower concentration ( $x \leq 0.05$ ) segregates at the grain boundaries of the conducting LCMO and raises the height of the tunnel barrier and subsequently impedes transport between the FM LCMO grains. But at higher concentration,  $x \geq 0.10$ , it forms a cluster along with the other reaction products in the LCMO matrix thereby improving the grain connectivity between LCMO and hence the conductivity of the system. This effect is pronounced in the MR behaviour of the system as shown in figure 8. The field-dependent resistivity of the system is measured under an applied field of 50 kOe from 5–300 K. All the composites show higher magnitude ( $\sim 87\%$ ) of MR compared to pure LCMO (46%); MR is highest (94%) for  $x = 0.05$  at the transition temperature. MR behaviour of the composite with 5 mol.% of  $\text{ZrO}_2$  is interesting. It peaks at  $T_C$  and remains constant at around 94% up to 75 K and goes down to around 85% below this. This near constancy below  $T_C$  has also been reported in CMR composite system LCMO:  $\text{SrTiO}_3$ <sup>16</sup> and could be useful from an application point of view. The enhancement of MR and its constancy up to low temperatures could be ascribed to magnetically disordered regions near the grain boundaries of LCMO. Because of the secondary phases the separation between conducting LCMO grains may become comparable to spin memory length.<sup>22</sup> If the effect is only due to magnetically disorder regions near the grain boundary, spin-dependent scattering

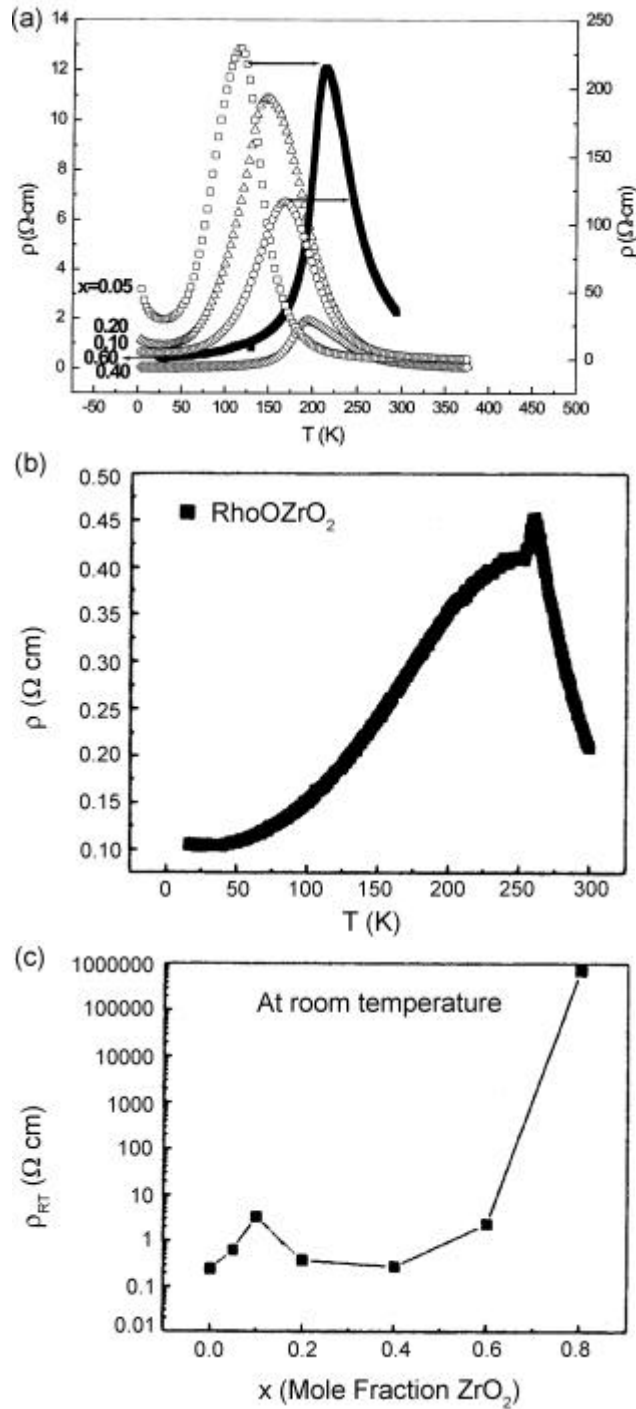


**Figure 7.** (a) Zero-field resistivity behaviour with temperature for  $\text{ZrO}_2$  composites. Right Y axis is for  $x = 0.05$  and  $0.10$ . (b) Shows the resistivity behaviour of the undoped compound ( $x = 0.0$ ), and (c) is room temperature resistivity behaviour with composition.

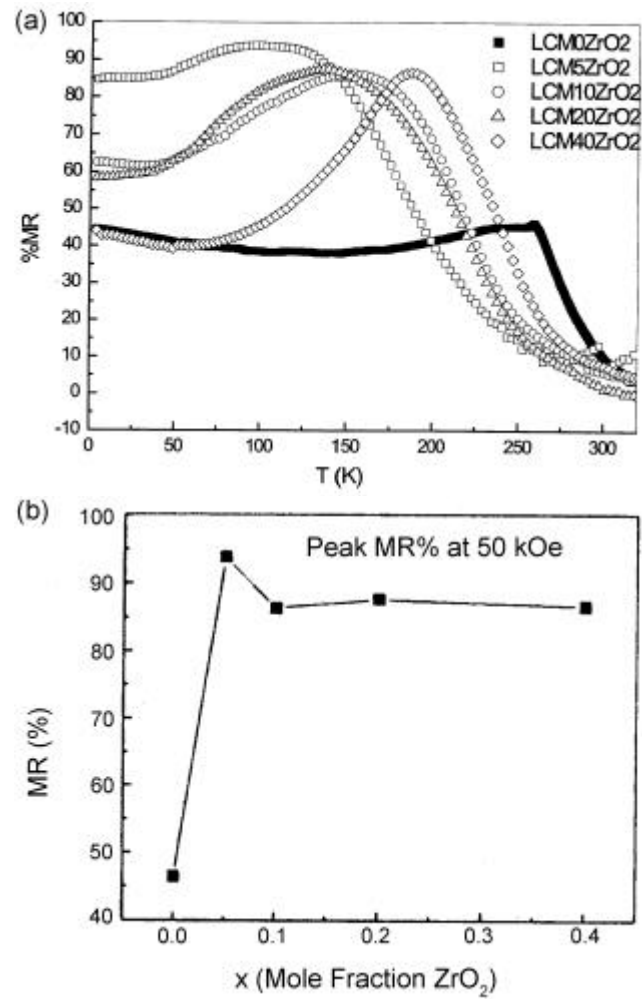


**Figure 8.** (a) Variation of %MR with temperature for ZrO<sub>2</sub> composites. (b) Peak MR behaviour with compositions,  $x$ .

(which may be temperature-dependent) could be essentially responsible for high MR and near temperature-independence below  $T_C$ . The behaviour of the composite with 40 mol.% ZrO<sub>2</sub>, however, is little different than the other composites. It shows a comparatively sharper peak in the MR curve around the transition temperature and the low temperature MR is smaller than that of the pure compound. For this composite the LCMO grain connectivity is much better compared to others, since the insulating phases segregate as a separate cluster. Spin-spin scattering at the transition temperature is responsible for the peaking nature and the different spin orientation in the insulating cluster is the reason for the low temperature MR behaviour, since the low temperature transport is controlled by the impurity scattering.

3.4 Properties of LCMO:  $x$ SiCN composites

LCMO:  $x$ SiCN ( $x$  = vol.% SiCN added) composites show almost similar behaviour to that of LCMO:  $x$ SiO<sub>2</sub> systems. XRD pattern of the composites show the presence of insulating Ca<sub>2</sub>La<sub>8</sub>(SiO<sub>4</sub>)<sub>6</sub>O<sub>2</sub> phase along with the LCMO reflections and which gets prominent as  $x$  increases. The shifting of the LCMO lines compared to the undoped compositions suggests the chemical reaction between the two phases. Magnetisation measurements (using a Quantum Design MPMS 7 SQUID) at an applied field of 5 kOe in the temperature range 5–300 K suggests that Si<sup>+4</sup> enters the LCMO lattice, since no shifting in the ferromagnetic transition temperature,  $T_C$  is observed with composition as shown in figure 9. Saturation magnetisation at 5 K falls with composition ( $x$ ) as expected

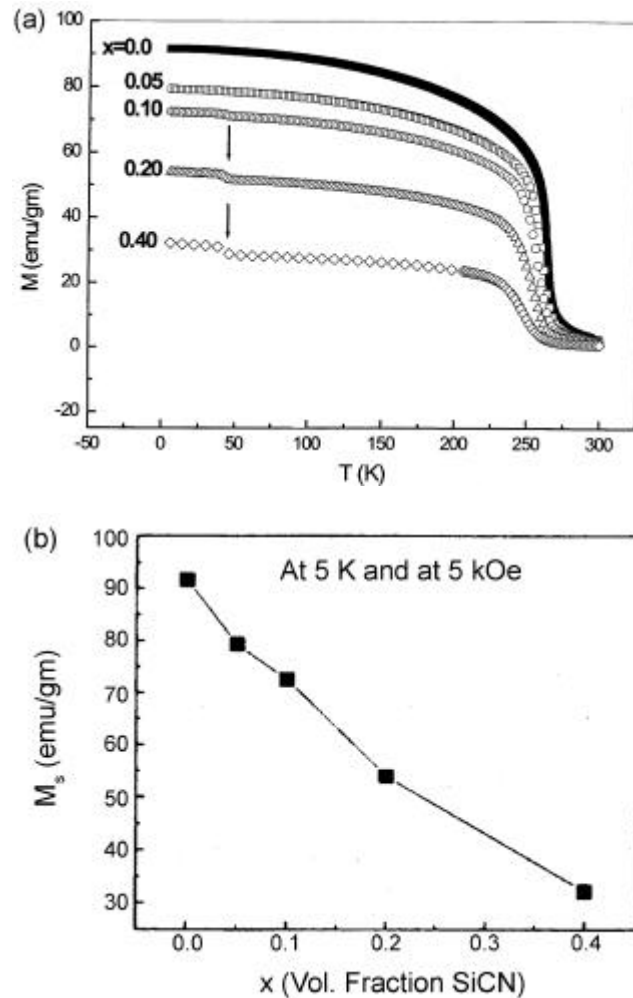


**Figure 9.** (a) Magnetisation behaviour of SiCN composites with temperature. (b) Saturation magnetisation,  $M_s$ , variation with compositions at 5 K and at 5 kOe field.

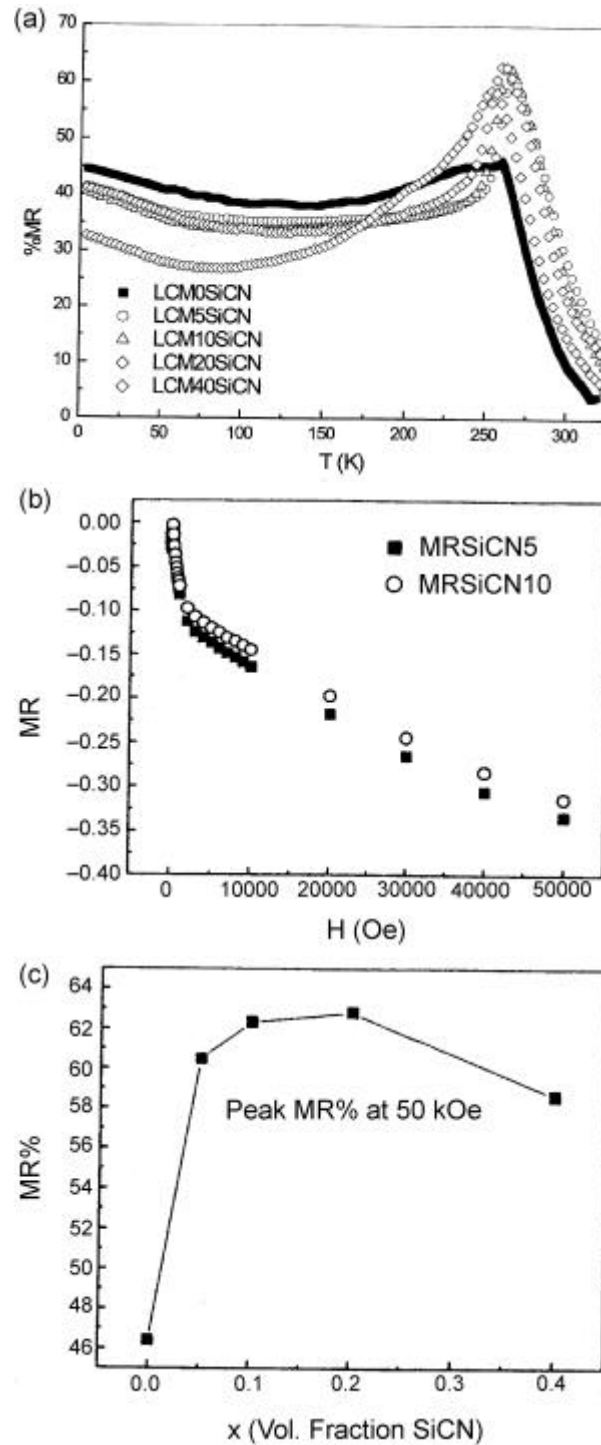


**Figure 10.** (a) Magnetoresistivity (%MR) behaviour of the SiCN composites with temperature. (b) Magnetic field dependence of MR for  $x = 0.05$  and  $0.10$ . (c) is variation of peak MR% with volume fraction of SiCN.

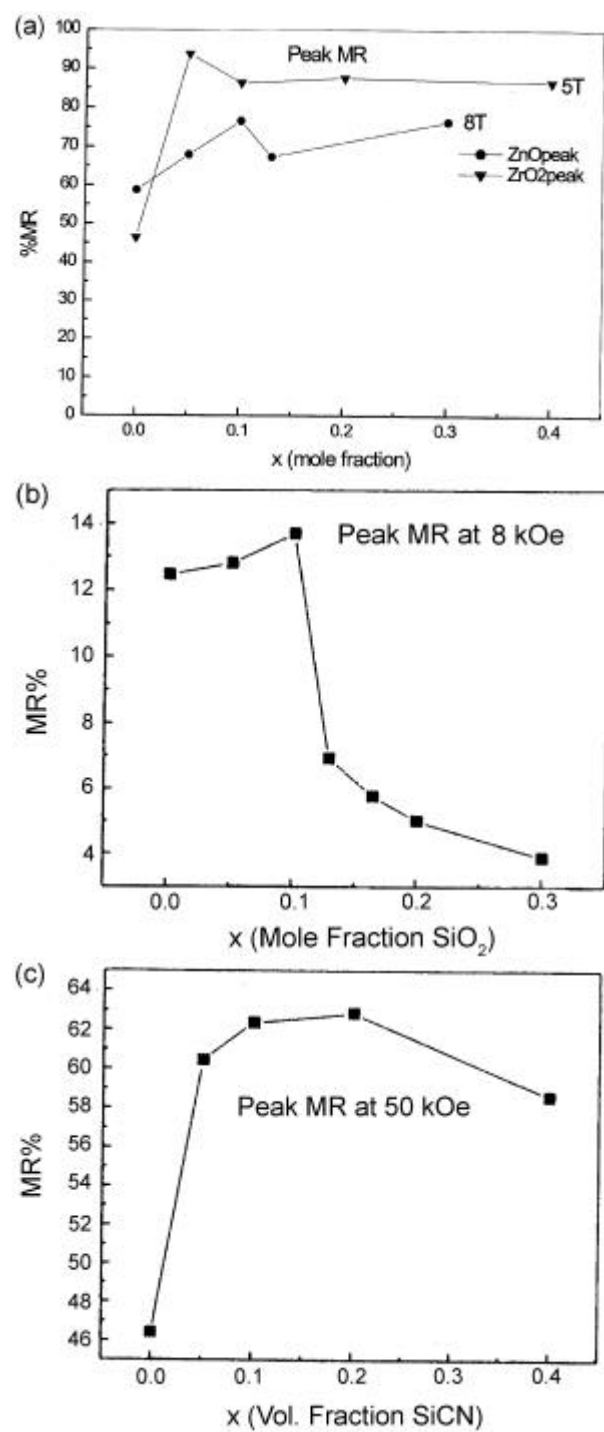


**Figure 11.** (a) Variation of peak magnetoresistivity (%MR) with compositions (mol. fraction/vol. fraction) for different composites. Same behaviour for SiO<sub>2</sub>(b) and SiCN (c) composites.

due to the magnetic dilution of the system in the presence of nonmagnetic silicate and is plotted in the inset of figure 9. However, the electrical transport properties are little different compared to LCMO:  $x\text{SiO}_2$  system. The resistivity of the system increases with increasing  $x$  due to the presence of insulating silicate in the grain boundaries of conducting LCMO but we do not find any percolation within the composition range studied. All the compositions show a distinct metal insulator transition slightly below their respective magnetic transition temperature. The MR behaviour (at 50 kOe) with temperature (shown in figure 10) shows the same trend as that of LCMO:  $x\text{SiO}_2$  composites. A maxima at  $T_C$  followed by a low temperature rising part attributed to the magnetic field-induced suppression of the spin-dependent scattering of the spin-polarised conduction electrons at the grain boundaries of LCMO phase. The magnetic field dependence of MR has been plotted in figure 10b for the compositions  $x = 0.05$  and  $0.10$ . The low field MR behaviour supports the grain boundary scattering of the conduction electron. Mahendiran *et al*<sup>43</sup> have observed the similar effect of low field MR behaviour for their pure LCMO and have explained the low field region as arising from the motion of the domain walls and the high field region from the gradual increase of the spontaneous magnetisation on application of the magnetic field. All the composites show higher magnitude of MR compared to pure LCMO ( $x = 0.0$ ) close to their magnetic transition temperature. Since the MR behaviour at the transition temperature is governed by the spin-spin scattering, the observed effect is expected. Variation of the peak MR with composition has been plotted figure 10b. However, low temperature MR of pure LCMO is substantially higher than that of the composites. Since the low temperature transport is governed by impurity scattering, different spin orientation in the insulating cluster is responsible for the low MR of the composites compared to pure LCMO at the low temperature region.

In figure 11 we have compared the magnitude of peak MR with compositions ( $x$ ) for all the systems studied by us. A maxima is observed for all systems at near the threshold composition. This could be used to further improve the LFMR properties of the composites.

#### 4. Conclusions

Increase in low field magnetoresistance (LFMR) over a wide range of temperature, or increase in room temperature MR, has been possible through microstructural tuning in different composites. Here the transport is mainly dominated by the temperature-dependent intergrain spin-polarised tunnelling of the conduction electrons between the FM grains across their grain boundaries particularly when the insulating layer is thin. But in case of thick layer the transport is dominated by the temperature-independent impurity scattering at the surface of the FM grains. This is more pronounced compared to the intrinsic effect which basically comes from the intergrain magnetic and transport properties caused by the double exchange between the neighbouring Mn ions in different valence states. CMR composites, compared to the pure CMR oxide systems like A or B site-doped  $\text{Ln}_{1-x}\text{Ca}_x\text{MnO}_3$  ( $\text{Ln} = \text{lanthanides}$ ), provide a means to take extrinsic CMR an upper hand over the intrinsic one. Since the extrinsic CMR is largely dependent on the grain boundary properties, a careful control of the microstructure of these composites may push a substantial LFMR towards room temperature, making these bulk composites suitable for potential device applications.

### Acknowledgement

We are grateful to Prof. C M Srivastava of IIT Bombay for many helpful discussions. We also thank to Prof. R Raj and Mr A Saha of the Department of Mechanical Engineering, University of Colorado at Boulder, USA and Dr S Russek of Magnetic Thin Films and Devices Sections at National Institute of Standards and Technology, Boulder, USA for conducting many experiments at their laboratories. Financial support from Department of Science and Technology, Govt. of India is gratefully acknowledged.

### References

1. Rao C N R and Raveau B (eds) 1998 *Colossal magnetoresistance, charge ordering and related properties of manganese oxides* (Singapore: World Scientific)
2. Jin S, Tiefel T H, McCormack M, Fastnach R A, Ramesh R and Chen L H 1994 *Science* **264** 413
3. Zener C 1951 *Phys. Rev.* **82** 403
4. Gupta A and Sun J Z 1999 *J. Magn. Magn. Mater.* **200** 24
5. Fontcuberta J, Bibes M, Martinez B, Trtik V, Ferrater C, Sanchez F and Varela M 2000 *J. Magn. Magn. Mater.* **211** 217
6. Issac S P, Mathur N D, Evetts J E and Blamire M G 1998 *Appl. Phys. Lett.* **72** 2038
7. Jin S, Tiefel T H, McCormack M, O'Bryan H M, Chen L H, Ramesh R and Schurig D 1995 *Appl. Phys. Lett.* **67** 557
8. Steren L B, Sirena M and Guimpel J 2000 *J. Magn. Magn. Mater.* **211** 28
9. Gong W Z, Zhao B R, Cai C and Lin Y 2001 *Appl. Phys. Lett.* **79** 827
10. Hwang H Y, Cheong S W, Ong N P and Batlogg B 1996 *Phys. Rev. Lett.* **77** 2041
11. Balcells L I, Carrillo A E, Martinez B and Fontcuberta J 1999 *Appl. Phys. Lett.* **74** 4014
12. Petrov D K, Krusin-Elbaum L, Sun J Z, Feild C and Duncombe P R 1999 *Appl. Phys. Lett.* **75** 995
13. Xia Z C, Yuan S L, Zhang L J, Zhang G H, Feng W, Tang J, Liu L, Liu S, Liu J, Peng G, Li Z Y, Yang Y P, Tang C Q and Xiong C S 2003 *Solid State Commun.* **125** 571
14. Huang Yun-Hui, Yan Chun-Hua, Wang Sa, Luo Feng, Wang Zhe-Ming, Liao Chun-Sheng, and Xu Guang-Xian 2001 *J. Mater. Chem.* **11** 3296
15. Hueso L E, Rivas J, Rivadulla F and López-Quintela M A 2001 *J. Appl. Phys.* **89** 1746
16. Hueso L E, Rivas J, Rivadulla F and López-Quintela M A 2001 *J. Non-Cryst. Solids* **287** 324
17. Köster S A, Moshnyaga V, Samwer K, Lebedev O I, Tendeloo G Van, Shapoval O and Belenchuk A 2002 *Appl. Phys. Lett.* **81** 1648
18. Shlyakhtin O A, Shin K H and Oh Young-Jei 2002 *J. Appl. Phys.* **91** 7403
19. Shlyakhtin O A, Oh Young-Jei and Tretyakov Yu D 2001 *Solid State Commun.* **117** 261
20. Yan Chun-Hua, Xu Zhi-Gang, Zhu Tao, Wang Zhe-Ming, Cheng Fu-Xiang, Huang Yun-Hui, and Liao Chun-Sheng 2000 *J. Appl. Phys.* **87** 5588
21. Huang Q, Li J, Huang X J, Ong C K and Gao X S 2001 *J. Appl. Phys.* **90** 2924
22. Gupta S, Ranjit R, Mitra C, Raychaudhuri P and Pinto R 2001 *Appl. Phys. Lett.* **78** 362
23. Huang Yun-Hui, Chen Xing, Wang Zhe-Ming, Liao Chun-Sheng, Yan Chun-Hua, Zhao Hong-Wu and Shen Bao-Gen 2002 *J. Appl. Phys.* **91** 7733
24. Yan Chun-Hua, Huang Yun-Hui, Chen Xing, Liao Chun-Sheng and Wang Zhe-Ming 2002 *J. Phys.* **14** 9607
25. Hong Chang Seop, Kim Wan Seop and Hur Nam Hwi 2002 *Solid State Commun.* **121** 657
26. Yan Chun-Hua, Luo Feng, Huang Yun-Hui, Li Xiao-Hang, Wang Zhe-Ming, Liao Chun-Sheng, Zhao Hong-Wu and Shen Bao-Gen 2002 *J. Appl. Phys.* **91** 7406
27. Liu J-M., Yuan G L, Sang H, Wu Z C, Chen X Y, Liu Z G, Du Y W, Huang Q and Ong C K 2001 *Appl. Phys. Lett.* **78** 1110
28. Yuan G L, Liu J-M, Liu Z G, Du Y W, Chan H L W and Choy C L 2002 *Mater. Chem. Phys.* **75** 161
29. Huang Yun-Hui, Yan Chun-Hua, Luo Feng, Song Wei, Wang Zhe-Ming and Liao Chun-Sheng 2002 *Appl. Phys. Lett.* **81** 76
30. Tang T, Zhang S Y, Huang R S and Du Y W 2003 *J. Alloy Compounds* **353** 91

31. Li Xiao-Hang, Huang Yun-Hui, Wang Zhe-Ming and Yan Chun-Hua 2002 *Appl. Phys. Lett.* **81** 307
32. Shannon R D and Prewitt C T 1969 *Acta Crystallogr.* **B25** 925
33. Das D, Chowdhury P, Das R N, Srivastava C M, Nigam A K and Bahadur D 2002 *J. Magn. Mater.* **238** 178
34. Das D, Saha A, Russek S E, Raj R and Bahadur D 2003 *J. Appl. Phys.* **93** 8301
35. Gebhardt J R, Roy S and Ali N 1999 *J. Appl. Phys.* **85** 5390
36. Walsh M C, Foldeaki M, Giguere A, Bahadur D, Mandal S K and Dunlap R A 1998 *Physica* **B253** 103
37. Bahadur D, Yewondwossen M, Koziol Z, Foldeaki M and Dunlap R A 1996 *J. Phys.* **8** 5235
38. Ju H L and Sohn Hyunchul 1997 *J. Magn. Mater.* **167** 200
39. Das R N, Das D, Srivastava C M, Nigam A K, Chowdhury P and Bahadur D 2000 Ferrites. In *Proc. 8th Int. Conf. on Ferrites (ICF 8)* (Kyoto and Tokyo) p. 250
40. Das D, Srivastava C M, Malik S K, Nigam A K and Bahadur D 2003 in *Magnetic and electrical transport properties of LCMO: ZnO composites* (to be published)
41. Ghosh K, Ogale S B, Ramesh R, Greene R L, Venkatesan T, Gapchup K M, Bathe Ravi and Patil S I 1999 *Phys. Rev.* **B59** 533
42. Xia Z C, Yuan S L, Tu F, Tang C Q, Peng G, Zhang G Q, Liu L, Liu J, Li Z Y, Yang Y P, Xiong C S and Xiong Y H 2002 *J. Phys.* **35** 177
43. Mahendiran R, Tiwary S K, Raychaudhuri A K, Ramakrishnan T V, Mahesh R, Rangavittal N and Rao C N R 1996 *Phys. Rev.* **B53** 3348